High-spin states in ^{214}Rn, ^{216}Ra and a study of even-even $N=128$ systematics

T. Lönnroth*
Brookhaven National Laboratory, Upton, New York 11973
and Department of Physics, University of Jyväskylä, Nisulankatu 78,
SF-40720 Jyväskylä 72, Finland

D. Horn, C. Baktash, and C. J. Lister†
Brookhaven National Laboratory, Upton, New York 11973

G. R. Young‡
Brookhaven National Laboratory, Upton, New York 11973
and Oak Ridge National Laboratory, Oak Ridge, Tennessee 37830
(Received 2 July 1982)

High-spin states in ^{214}Rn and ^{216}Ra have been studied by means of the reaction ^{208}Pb(^{13}C, α $3n$ γ)^{214}Rn and ^{208}Pb(^{13}C, $5n$ γ)^{216}Ra at beam energies in the range 75–95 MeV. In-beam spectroscopy techniques, including γ-decay excitation functions, α-γ coincidences, γ-γ coincidences, γ-ray angular distributions, and pulsed-beam-γ timing, were utilized to establish level energies, γ-ray multipolarities, J^π assignments, and isomeric lifetimes. Excited states with spins up to $23\hbar$ in ^{214}Rn and $\sim 30\hbar$ in ^{216}Ra were observed. Isomers were found in ^{214}Rn at 1625 keV ($T_{1/2}=9$ ns, $J^\pi=8^+$), 1787 keV (22 ns, 10^+), 3485 keV (95 ns, 16), 4509 keV (230 ns, 20), and 4738 keV (8 ns, 22), and in ^{216}Ra at 1708 keV (8 ns, 8^+) and 5868 keV (10 ns, ~ 24). $B(EL)$ values were deduced and compared to previously known lead-region electric transition rates. Shell-model calculations were performed and used to make configurational assignments. The absence of major α-decay branching in the isomers is explained and the systematic behavior of $N=128$ even-even nuclei is discussed.

NUCLEAR STRUCTURE ^{208}Pb(^{13}C,α $3n$ γ)^{214}Rn, ^{208}Pb(^{13}C,$5n$ γ) ^{216}Ra, $E_{\rm lab}=75-95$ MeV. Measured α-γ coin, γ-$\gamma(t)$ coin, $I(\theta)$, pulsed-beam-γ timing. Deduced level schemes, J^π, $T_{1/2}$, $B(EL)$, multipolarities. Shell model calculations, Ge(Li) and Si detectors, enriched target.

I. INTRODUCTION

The shell-model concept of effective two-nucleon interactions[1] has been successful in describing properties of "magic" nuclei, i.e., nuclei with N or Z equal to 20, 28, 50, (64), 82, or 126. It is thus found that nuclei around ^{208}Pb with $Z\approx 82$ and $N\approx 126$ can successfully be described in terms of effective interactions. This approach has been taken in a number of recent experimental and review articles (Refs. 2–8, and references therein). However, little of this work has involved nuclei with valence neutrons outside the $N=126$ core, due largely to the difficulty of producing these nuclei for in-beam study. The present study of the $N=128$ isotones $^{214}_{86}$Rn and $^{216}_{88}$Rn should therefore serve as a test of the shell model in this region, especially at high spins.

^{214}Rn and ^{216}Ra are the $N=128$ isotones with four and six valence protons, respectively, relative to the ^{208}Pb core. The high spin single particle orbitals available to these valence nucleons are known from the observed spectra of ^{209}Bi (for protons) and ^{209}Pb (for neutrons)[9]; they are the following:

$$\pi{:}1h_{9/2}(0\ \text{keV});2f_{7/2}(896\ \text{keV})\ ;$$
$$1i_{13/2}(1609\ \text{keV})\ ,$$
$$\nu{:}2g_{9/2}(0\ \text{keV});1i_{11/2}(779\ \text{keV})\ ;$$
$$1j_{15/2}(1423\ \text{keV})\ .$$

The strongly attractive proton-neutron effective interaction[1,8] is especially important for high spin states on and near the yrast line, as it significantly lowers the excitation energy of those levels with aligned high-j components. One may estimate the maximum spin attributable to those aligned configurations to be of the order of $J\sim 33$ with a wave function, for example, of

$$\pi(h_{9/2}{}^2 i_{13/2}{}^2)_{20^+} \otimes \nu(i_{11/2} j_{15/2})_{13^-} .$$

However, it is probable that core excitations begin to contribute significantly to these higher spin states.

Prior to the present work, nuclear structure information on lighter $N=128$ isotones[6,10,11] (^{210}Pb, ^{212}Po, and ^{213}At) has been obtained from α and ^{7}Li-induced reactions. For ^{214}Rn only the α-decaying ground state ($T_{1/2}=270$ ns, $\alpha_0=9.04$ MeV) was known[12] until, recently, its low-lying states to spin 8 were established.[13] Studies of ^{216}Ra [$T_{1/2}=180$ ns, $\alpha_0=9.35$ MeV (Ref. 14)] to a possible spin $J^\pi=14^+$ and excitation energy 3292 keV have revealed several alpha-decaying states.[15]

The experimental procedure and data reduction techniques used in the present work are described in Sec. II and the resulting level schemes are presented in Sec. III. In Sec. IV we outline the shell model theoretical calculations which serve as a basis for suggested configuration assignments and for the theoretical $B(\lambda)$ and Γ_α values. Finally, in Sec. V we compare the systematical behavior of $N=128$ even-A nuclei with that of the previously studied corresponding $N=126$ nuclei.[5] In Sec. V we also discuss the implications of the deviations of the $B(\lambda)$ values from the Weisskopf estimates and we draw conclusions regarding the nuclear intrinsic structures.

II. EXPERIMENTAL PROCEDURE AND DATA ANALYSIS

Levels in the nuclei ^{214}Rn and ^{216}Ra were populated in the reactions of ^{13}C beams with enriched ($>99\%$), thick (6 mg/cm^2), self-supporting targets of ^{208}Pb at the Brookhaven tandem Van de Graaff facility. Fusion-evaporation channels appeared to prevail over the fission channel in the reactions studied, so that the yields of the desired residual nuclei were adequate. Gamma rays were detected with coaxial Ge(Li) detectors of 21% efficiency and 1.9 keV resolution (FWHM) at 1332 keV. A sample singles spectrum for reactions induced by 90 MeV ^{13}C is shown in Fig. 1.

For the excitation function measurements, the energy of the ^{13}C beam was varied from 75 to 95 MeV in steps of 5 MeV and the γ-ray yields were normalized to the integrated beam current. The resulting yield curves for transitions characteristic of ^{216}Ra and ^{214}Rn are shown in Fig. 2. The peak yields for both $5n$ and $\alpha\, 3n$ evaporations were found at the laboratory energy of approximately 86 MeV. The fixed energy measurements were then made at 90 MeV, a slightly higher energy, in order to enhance the production of high spin states without excessive loss of cross section.

In order to discern between γ rays belonging to ^{214}Rn and those belonging to ^{216}Ra, α-γ coincidence measurements were performed. This was possible since the ground state half-lives of 270 and 180 ns,

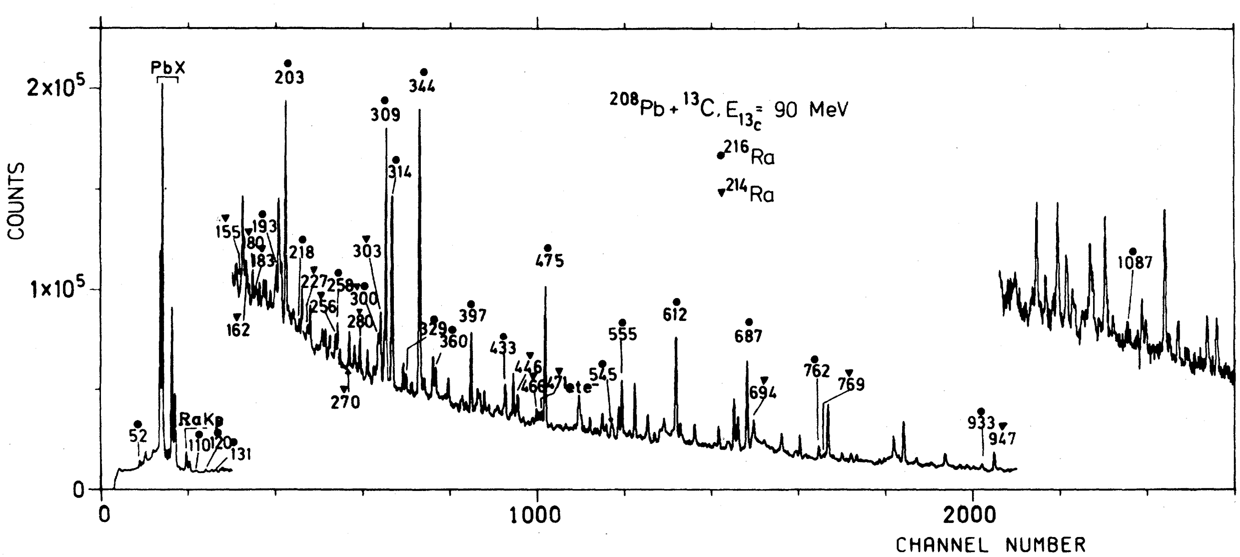

FIG. 1. Singles spectrum from the reaction ^{13}C + ^{208}Pb at 90 MeV.

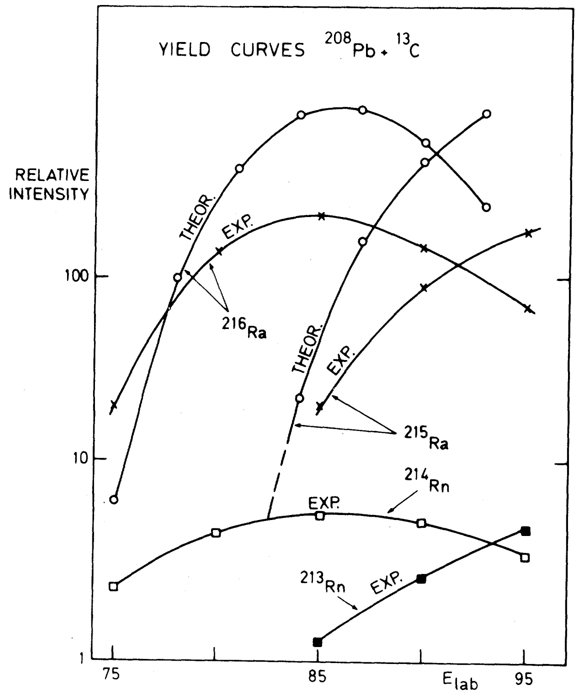

FIG. 2. Yield curves for transitions assigned to ^{215,216}Ra and ^{213,214}Rn. A comparison is made with the predictions of the fusion-evaporation code GROGI (Ref. 39). The experimental and theoretical curves are not mutually normalized.

respectively, were short enough to allow for a substantial coincidence rate. The alpha particles were detected in a silicon surface barrier detector, 150 μm thick and 150 mm^2 in area. The singles alpha-particles spectra show strong α groups from ^{214}Rn and ^{216}Ra and weak ones from ^{213}Rn and ^{215}Ra. The $\alpha_0=9.04$ MeV ground state decay of ^{214}Rn was seen in coincidence with γ lines attributed to this nucleus and similarly $\alpha_0=9.35$ MeV for γ rays in ^{216}Ra. The previously reported[15] high energy alpha groups were also seen, and their branching intensity, $<1\%$, put an upper limit for the α-decay branching of high-spin levels observed in this work.

In order to confirm the Z assignments of the γ rays, coincidences between x rays and γ rays were studied. Figure 3 shows radon x rays in coincidence with gamma rays presumed to be transitions in ^{214}Rn, and Fig. 4 shows radium x rays coincident with lines in ^{216}Ra. Thus three independent methods, α-γ coincidences, excitation functions, and x-γ coincidences, were used in the assignment of γ rays to either ^{214}Rn or ^{216}Ra.

Gamma-gamma coincidences were measured with two Ge(Li) detectors placed at angles of 90° and 125° with respect to the beam direction. Both were shielded by 0.5 mm Cu absorbers. The energy signal from each detector and the time between the two were recorded in an event-by-event mode. Dividing the relative time spectrum into three regions (cf. inset of Fig. 3) made it possible to categorize the coincident gamma rays by their arrival time with respect to the gating transition. If a nucleus has an isomer with a lifetime longer than the electronic resolution time (~ 15 ns) then clear "before-prompt-after" relations can be established which are invaluable in ordering partial cascades of transitions. This was the case in ^{214}Rn. Spectra gated by γ rays in ^{214}Rn are displayed in Fig. 3. Various panels show the transitions preceding the gating transition, those in prompt coincidence (± 15 ns) with it, and transitions coming after the gate. In ^{216}Ra the half-lives of the isomers are of the order of the electronic resolution time and γ-γ coincidences cannot be used to establish their timing relationships. Figure 4 shows gated spectra of γ rays belonging to ^{216}Ra: panel (b) is a sum gate of uncontaminated transitions previously assigned[15] to ^{216}Ra, and panels (a) and (c) show gates on some relevant transitions assigned in this work to ^{216}Rn.

Isomeric lifetimes were measured with the ^{13}C beam pulsed at a repetition rate of 2 μs with a pulse width of about 10 ns. The time curves were fitted to multiple-level decay formulae. In Fig. 5 we present examples of time curves for transitions assigned to ^{214}Rn.

The angular distribution measurements were made at 90 MeV beam energy and for eight angles in the angular interval 60°—158° with respect to the beam direction with a fixed monitor detector. To average out the variations due to beam fluctuations, the measurements were divided into ten cycles, each lasting 80 min. The total beam current, simultaneously recorded for each angle, served as an additional normalization. It was found that the difference between the two normalizations was less than 1%. The peak areas were fitted to a truncated Legendre polynomial, giving γ-ray intensities and A_2/A_0 and A_4/A_0 coefficients. A test of χ^2 was performed for a simultaneous fit of multipole mixing. Properties of the gamma rays observed in ^{214}Rn and ^{216}Ra are summarized in Tables I and II, respectively.

III. THE LEVEL SCHEMES of ^{214}Rn and ^{216}Ra

A. ^{214}Rn

The level scheme of ^{214}Rn is presented in Fig. 6. The partial level scheme up to $J^\pi=8^+$ as reported

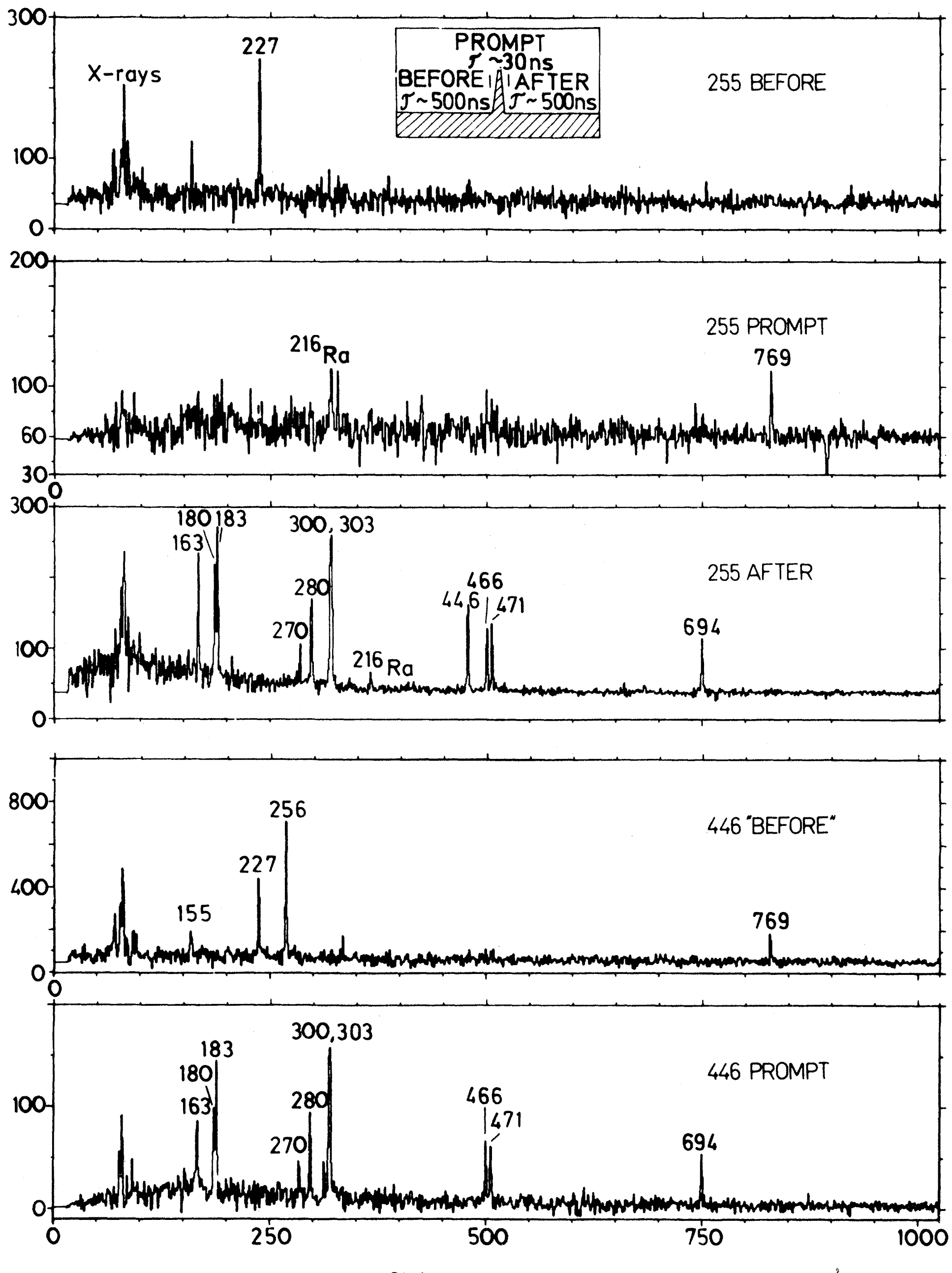

FIG. 3. Background-subtracted coincidence spectra for transitions assigned to ^{214}Rn. The inset shows the time windows used for dividing the coincidences into "prompt-before-after" categories.

in Ref. 13 was confirmed. The construction of the level scheme was largely facilitated by the presence of the isomers which allowed the establishment of partial cascades. Whenever possible, coincidence γ-ray intensities were used as an additional constraint to remove ambiguities in the level ordering. That is, we took advantage of the fact that in spectra projected from a given gating transition, intensities of the transitions originating from the higher lying states follow the singles intensities. In contrast, γ rays lying below the gating transitions are reduced relative to their singles intensities, as sidefeeding to the lower levels is not observed. In addition, when the absolute γ-ray coincidence intensities are measured, the cascades lying below the gating transition should all have the same intensity

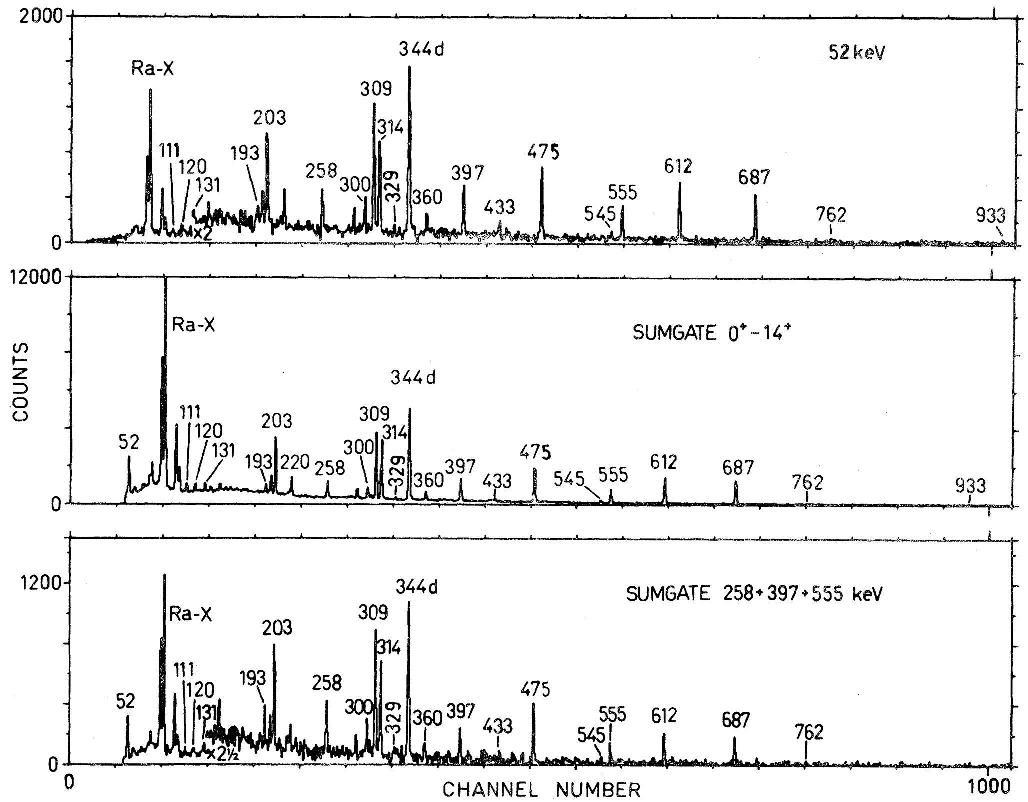

FIG. 4. Background-subtracted coincidence spectra for transitions in ^{216}Ra. Shown are the sum gate of lines reported previously (Ref. 15) (middle panel) and gates on some of the strongest new lines (bottom panel).

when electron conversion is taken into account. Indeed, in cases where the one-to-one ratio is not observed, the degree of electron conversion can be estimated. Frequently this method can be used to differentiate between electric and magnetic decay, especially in the case of low energy transitions.

Angular distribution data were utilized to determine the transition multipolarities. Moreover, lifetimes provided additional information concerning the character of the depopulating transitions. For example, a $T_{1/2}=230$ ns lifetime for the $J=20$ state indicates a strength of 12 or 1.2×10^{-4} W.u. for the 768.9 keV transition if we assume an $E3$ or $E2$ character, respectively. The latter hindrance factor is outside the systematics of the observed $E2$ transition rates. A similar argument leads to an $E2$ assignment for the 947.1 keV γ ray. (An $M2$ character gives a lifetime of $T_{1/2}\geq 5$ ns for the $J=12$ state, assuming the fastest observed $M2$ transition rate.)

Requiring an intensity balance at the $J=12$ and 13 states implies electric character for 270.1, 280.4, and 300.4 keV transitions. This results in the assignment of $12^{(+)}$, $12^{(+)}$, and $13^{(-)}$ for the states at 2734, 2724, and 3004 keV excitation energy, respectively. The ordering of 471.1- and 465.8-keV dipole transitions could not be determined.

On the basis of the observed half-life for the $J=16$ state (95 ns), both $E2$ and $M2$ assignments are possible for the 180.3 keV transition (Weisskopf estimates are 30 and 125 ns, respectively.) The corresponding conversion factors, however, differ by a factor of 17, thus eliminating the possibility of $M2$. On the basis of its intensity, the 255.5 keV gamma ray was assigned an $E1$ character (nearly 5% electron converted for an $E1$ as compared to 95% for $M1$), and placed below the 768.9 keV transition. Further arguments in favor of this ordering are (i) lack of a prompt component in the decay curve of the 768.9 keV line; and (ii) the lifetime of the state.

The 227.4- and 155.0-keV gamma rays are the only prominent lines in the "before" gates (Fig. 3). From angular distribution data, their multipolarities were inferred to be quadrupole and dipole, respectively. Singles and coincidence intensities rule out an $M1$ choice (α_{tot} is 0.17, 1.6, and 8.3 for

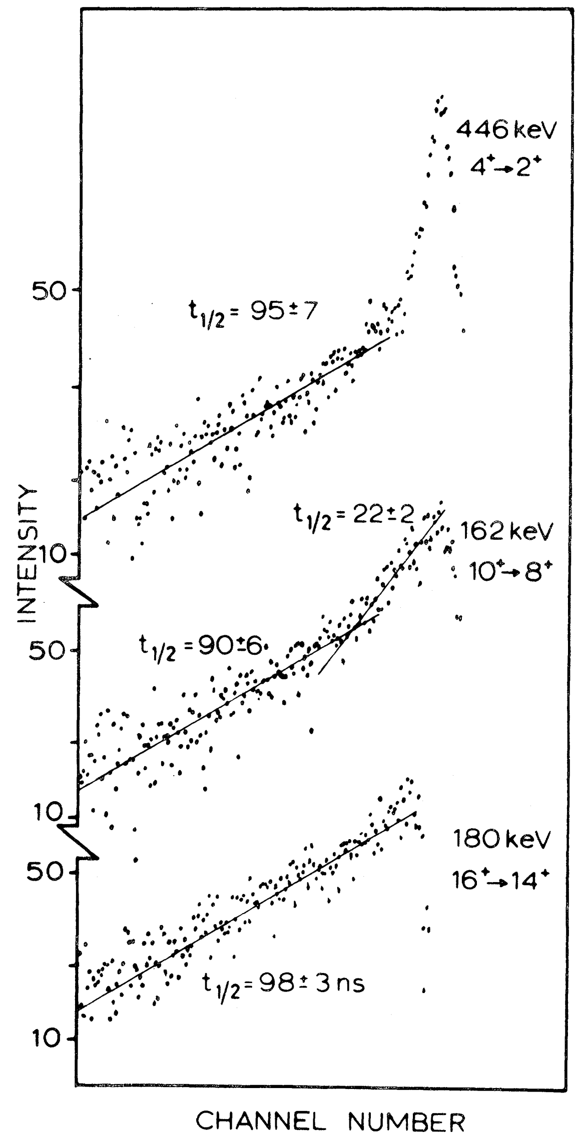

FIG. 5. Time curves for some transitions in ^{214}Rn and ^{216}Ra.

$E1$, $E2$, and $M1$, respectively) for the 155.0 keV line. Their ordering was decided on the basis of their relative intensities.

B. ^{216}Ra

The level scheme of ^{216}Ra is presented in Fig. 7. Levels to a tentative $J=14$ at 3288 keV have been reported previously[13,15] and our results are consistent with those assignments. The location of the $T_{1/2}=8.1$ ns isomer in the figure is taken from Ref. 15. Above the $J=14^+$ state, the level scheme was deduced using many of the techniques described for ^{214}Rn in the previous section.

Four conspicuous dipole transitions of 51.7, 555.2, 397.4, and 257.8 keV feed the $J=14^+$ state. The high conversion coefficients for low-energy magnetic transitions rule out a magnetic character for the 51.7-keV gamma ray. The difference between the electric and magnetic conversion coefficients for a 555.2-keV dipole transition is too small for a positive determination of that γ ray, leaving the parities uncertain for all levels with spins of 16 or greater.

Feeding the $J^\pi=18^{(+)}$ level is a cascade five dipole transitions whose relative ordering is uncertain. The 761.9-keV transition ($E2$ or $E3$) is crossed over by 329.4- and 433.1-keV gamma rays. A 110.7-keV dipole transition has been observed out of beam[16] with sufficient intensity to suggest $E1$ character. The three remaining dipole transitions are low in energy and have undetermined parity. Their location relative to the high spin isomer is not entirely certain due to their slow rise times as observed in the Ge(Li) detectors. Accordingly, the placement of the isomer at an excitation energy of 5868 keV and a spin of 24 is tentative.

The isomer is fed by three quadrupole transitions, 360.4, 300.4, and 217.7 keV in energy, which are all seen, and are the only ones seen, in the before time window of all lower-lying transitions. The absence of a delayed component in this cascade makes magnetic character unlikely for these three transitions. The $T_{1/2}=10\pm3$ ns half-life for the isomer is inferred from the intensity reduction in various γ-γ coincidence time windows and can also be estimated from the pulsed beam time distributions for transitions between the $J^\pi=8^+$ and 24 levels, after compensating for the width of the bunched beam.

IV. SHELL-MODEL CALCULATIONS

A. Level energies

The pioneering work of using effective two-body interactions in shell-model theory was done by deShalit and Talmi.[17] When it was realized that ^{208}Pb formed a remarkably inert core, the concept was applied by Blomqvist to nuclei in the lead region. Using empirical two-nucleon matrix elements rather than theoretical ones, considerable success has been achieved for few-nucleon cases (see, e.g., Refs. 2–4 for a review).

In this work we calculate the excitation energies for valence multiparticle configurations of the $(\pi^4\nu^2)$ and $(\pi^6\nu^2)$ type in ^{214}Rn and ^{216}Ra, respectively (π stands for proton and ν for neutron). For

TABLE I. Properties of gamma rays assigned to ^{214}Rn.

E_γ (keV)	I_γ[a]	A_2/A_0	A_4/A_0	$t_{1/2}$ (ns)[b]	Assignment[c]
155.0[d]	$\lesssim 10$				$E1$
162.0	44	0.02(3)	−0.03(5)	22(5)	$E2$
180.3	34	0.11(2)	−0.03(4)	116(15)	$E2$
182.5	31	0.12(1)	−0.06(3)	98(3)	$E2$
227.4	16	0.16(4)	−0.11(7)	8.0(3)	$E2$
255.5	42	−0.13(3)	0.04(5)	224(30)	$E1$
270.1	~20	−0.04(2)	−0.03(3)	113(16)	$E1$
280.4[d]	23	−0.15(7)	−0.01(13)	98(9)	$(E1)$
300.4[d]	~50	−0.29(3)	0.10(4)	90(5),231(15)	$(E1)$
302.5[d]	~65	0.05(3)	−0.02(6)		$E2$
446.0	79	0.09(3)	−0.03(6)	95(7)	$E2$
465.8	42	−0.19(5)	0.25(7)	101(6)	$\lambda=1$
471.1	48	−0.15(6)	0.16(10)	93(5)	$\lambda=1$
693.6	100	0.29(6)	−0.09(9)	97(5)	$E2$
768.9	29	0.18(6)	−0.01(10)	~250	$E3$
947.1[d]	24	>0	<0		$(E2)$

[a]Errors range from 5 to 10% depending on intensity.
[b]From fits to the respective time curves.
[c]Parities deduced indirectly from cascade intensities, or from half-life arguments.
[d]Doublet.

TABLE II. Properties of gamma rays assigned to ^{216}Ra[a].

E_γ (keV)	I_γ[b]	A_2/A_0	A_4/A_0	Multipole[c]
51.7	38	−0.31(1)	0.01(2)	$E1$
110.7	5	−0.20(4)	0.01(7)	$(E1)$
120.4	8	−0.27(3)	0.05(5)	$\lambda=1$
131.0	6	−0.05(1)	0.01(10)	$\lambda=1$
193.5	14	−0.29(1)	−0.00(3)	$\lambda=1$
203.5	68	0.20(5)	−0.10(5)	$E2$
217.7	4	0.26(4)	−0.09(7)	$E2$
257.8	15	−0.15(2)	0.06(4)	$\lambda=1$
300.4[d]	~5	0.12(1)	−0.10(3)	$E2$
308.7	105	−0.32(1)	0.01(2)	$E1$
314.5	90	0.25(4)	−0.07(5)	$E2$
329.4[d]	~5			
343.5+3.445[d]	~180	e	e	$E2$ both
360.4	6	0.27(3)	−0.08(4)	$E2$
397.4	48	−0.29(1)	0.01(2)	$\lambda=1$
433.1[d]	<20	−0.17(7)	−0.00(4)	$\lambda=1$
474.7	105	0.23(3)	−0.05(6)	$E2$
555.2	60	−0.32(2)	0.03(3)	$\lambda=1$
612.0	104	−0.32(1)	0.02(2)	$E1$
686.6	100	−0.01(2)	−0.08(4)	$(E2)$
761.9	~5	>0		$\lambda=2,3$

[a]Additional transitions were observed but are not included since they could not be placed in the level scheme.
[b]Errors are typically 5 to 10% depending on intensity.
[c]Parities deduced indirectly from cascade intensities; see the text.
[d]Doublet.
[e]Very strong positive $A2$ and negative $A4$; both components are quadrupoles.

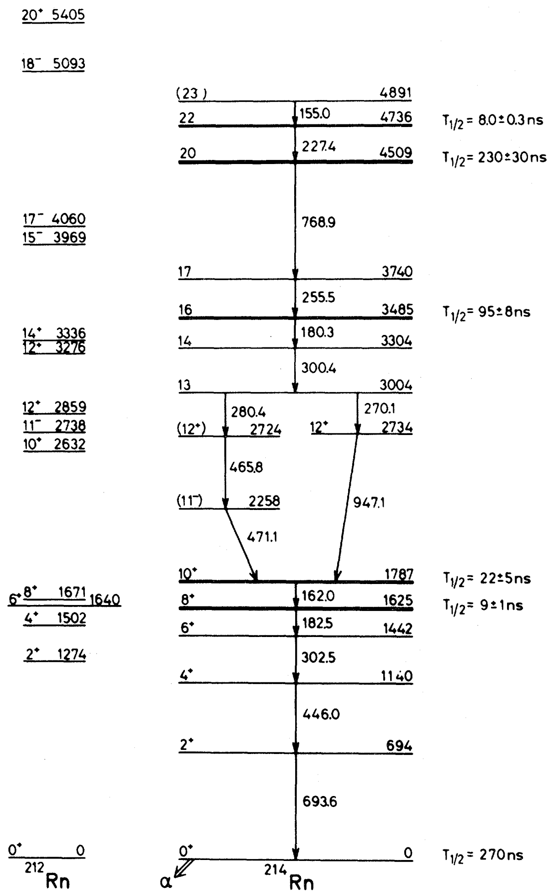

FIG. 6. The level scheme of ^{214}Rn as deduced in the present study. The ordering of the 471.1 and 465.8 keV transitions is not certain. On the left the yrast valence nucleon levels of ^{212}Rn, which provide the proton states, are displayed for comparison.

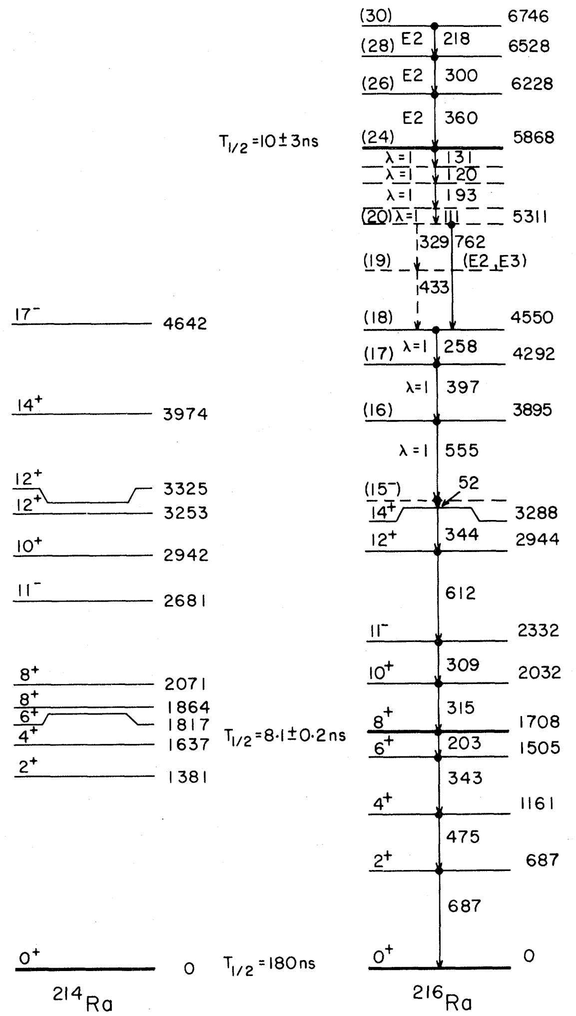

FIG. 7. The level scheme of ^{216}Ra as deduced in the present study. Uncertainties in relative ordering of transitions are indicated by dashed levels. On the left states of ^{214}Ra are displayed for comparison.

comparison we also indicate excitation energies of the particle-hole core-excited states. The yrast particle-hole excitations in proton-rich nuclei are of the form $|\nu\nu^{-1}\rangle$. The wave function for a core-excited state in ^{216}Ra would then be of the form $|\pi^6\nu^3\nu^{-1}\rangle$, involving ten particles. Since the experimental reaction yields information predominantly on high-spin yrast levels, only high-spin single-particle orbitals are included. The empirical interaction energy matrix elements can be obtained from experimentally determined two-nucleon spectra of ^{210}Pb(ν^2), ^{210}Pb(π^2), and ^{210}Bi($\pi\nu$), as discussed in Refs. 2 and 8. As an example, for a proton-neutron matrix element we have

$$\langle j_n j_p;J\,|\,V_{np}\,|\,j_n j_p;J\rangle$$
$$= -S_p(^{209}\mathrm{Bi}) - S_n(^{209}\mathrm{Pb}) - E_{\mathrm{exc}}(j_p;{}^{209}\mathrm{Bi}) - E_{\mathrm{exc}}(j_n;{}^{209}\mathrm{Pb}) + E_{\mathrm{exc}}(j_n j_p J;{}^{210}\mathrm{Bi})\ ,$$

where j_n (j_p) are the neutron (proton) orbitals, E_{exc} is the relevant excitation energy, and S_n (S_p) are the neutron (proton) separation energies.[18] When the empirical matrix elements are not known, those of Kuo and Herling[19] are used.

B. Transition rates

The expressions for the electric and magnetic L-pole reduced single-particle transition probabilities are well known.[17,20] The main inputs for calculating electric transitions are the radial integrals $|\langle R_f\,|\,r^L\,|\,R_i\rangle|^2$. For the simplifying assumption of $R_{i,f}=\mathrm{const}$ ($r \le a$) and $R_{i,f}=0$ ($r > a$) one gets the Weisskopf estimates. For a harmonic oscillator potential the integrals can be solved analytically. However, the orbitals in the lead region deviate by roughly 20% from the harmonic oscillator wave functions if, instead, a Woods-Saxon potential is used.[21] We calculate $E2$ and $E3$ transition probabilities using the radial wave functions of Ref. 21.

The alpha-decay widths can be derived from a model of Kadmenskij *et al.*[22] Correction factors may be introduced to account for the finite size of the α particle.[22] Results generally agree poorly with the data, since no exact theory is available.

V. DISCUSSION

A. $N=128$ level systematics

As mentioned in the Introduction, several attempts have been made to experimentally determine the properties of (high-spin) states in nuclei with proton particles and neutron holes around ^{208}Pb, but few for nuclei with both proton and neutron valence particles (Refs. 2–6 and 13). A detailed comparison for $N=126$ isotones, i.e., nuclei with N proton particles outside the ^{208}Pb core, was performed recently.[5] In this work we compare the experimentally determined behavior of $N=128$ isotones, that is nuclei with 2 neutron valence particles and N proton valence particles, as shown in Fig. 8. (For a comparison of experiment and theory, see Fig. 9.) It is clearly seen in Fig. 8 that some specific levels are pertinent to all isotones. Such are the 0^+-10^+ levels, interpreted to be mainly of the configuration $(g_{9/2}{}^2)_{0^+-8^+}$ and $(g_{9/2}i_{11/2})_{0^+-10^+}$ with the N protons coupled to $J=0^+$ though substantial mixing of $(h_{9/2})_{6^+-8^+}{}^2$ states may be expected. The 11^- levels at about 2300 keV are most probably due to the seniority-two proton configuration $(h_{9/2}i_{13/2})_{11^-}$, situated in the $N=126$ isotones at ≈ 2800 keV. The reduction in their energy by 500 keV in the $N=128$ isotones may be ascribed to the proton-neutron interaction which is strongly attractive.[8] In our calculation, the positive-parity yrast states, $J^\pi=12^+-16^+$, arise mainly from the coupling of two $h_{9/2}$ protons and two $g_{9/2}$ neutrons with spin values in the range 4^+-8^+.

There exists a $t_{1/2}=45$ s, α-decaying high spin isomer in ^{212}Po. If this state has $J=18^+$, the neutron part is most probably $(\nu g_{9/2}i_{11/2})_{10^+}$ (cf. Refs. 25 and 26). A spin value of 16^+, on the other hand, restricts the spin value of the level at 2480 keV to 12, since the $E4$ half-life is then of the order of 50 s. (A 13^+ level implying an ~ 500 keV $M3$ transition would result in a half-life of ~ 1 ms for a $16^+\rightarrow 13^+$ transition, greatly underestimating the half-life of the isomer.)

Higher-lying states in the $N=128$ isotones may be interpreted as arising from coupling the proton $(h_{9/2}i_{13/2})_{11^-}$ state to the neutron 0^+-10^+ states, whereas the $20^{(+)}$ and $22^{(+)}$ states in ^{214}Rn are proposed to be of the

$$(\pi h_{9/2}{}^4)_{12^+}\otimes(\nu g_{9/2}{}^2)_{8^+}$$

and

$$(\pi h_{9/2}{}^4)_{12^+}\otimes(\nu g_{9/2}i_{11/2})_{10^+}$$

configurations, respectively.

The states in the range $J=22-27$ (Fig. 9) can also be obtained from the configurations

$$(\pi h_{9/2}{}^3 i_{13/2})_{15^-,17^-}\otimes(\nu^2)_{6^+-10^+} ,$$

where the neutron parts are as given above, but these states seem to be nonyrast.

As seen in Fig. 9, the agreement between theory and experiment is satisfactory. The deviations are, with a few exceptions, of the order of 100 keV. This is of the same order as in a recent work on high-spin states in ^{211}Rn.[27]

B. Effective moment of inertia

Within the framework of the independent particle model, the excitation energies are expected to follow, on the average, the rigid rotor relationship

$$E^*=\frac{\hbar^2}{2\mathscr{I}_{\text{eff}}}J(J+1) .$$

The effective moment of inertia, $\mathscr{I}_{\text{eff}}$, therefore may be obtained from the slope of the yrast line in a plot of energy vs $J(J+1)$. Figure 10 represents such a plot for several nuclei in the $N\geq 126$, $Z\geq 82$ region. Pairing correlations, which are important for the low spin states, reduce the effective moment of inertia from the rigid rotor value. For example, the resulting $\mathscr{I}_{\text{eff}}$ is only half the rigid rotor value at spins $J\leq 16$ for the $N=126$ and 128 isotones. At higher spins, however, $\mathscr{I}_{\text{eff}}$ gradually increases and approaches the rigid rotor value of

$$\frac{2\mathscr{I}}{\hbar^2}\approx 200\ (\text{MeV})^{-1} .$$

C. Transition rates

It is interesting to compare $B(EL)$ values for states which have easily measurable half-lives (usu-

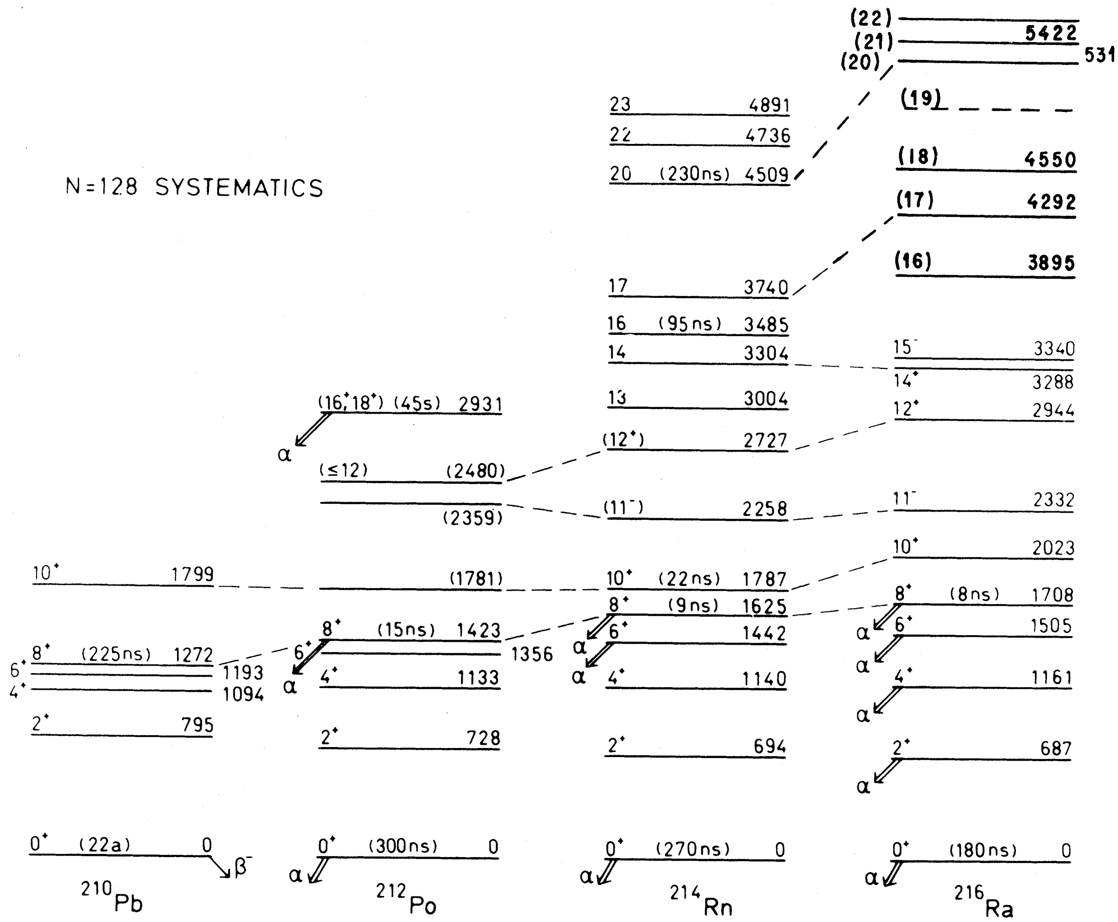

FIG. 8. Comparison of experimentally determined level schemes of the even-even $N=128$ isotones ^{210}Pb, ^{212}Po, ^{214}Rn, and ^{216}Ra. The level schemes of ^{210}Pb and ^{212}Po are from Refs. 6 and 24, respectively.

ally $t_{1/2}\geq 1$ ns), since transition rates are much more sensitive to structural changes than the excitation energies. We shall discuss the characteristics of electric dipole, quadrupole, and octupole transitions in the lead region and draw conclusions regarding transitions in the $N=128$ isotones.

Selected $E1$, $E2$, and $E3$ transitions observed in $Z\geq 82$, $N\geq 126$ nuclei are collected in Table III. It must be noted that, by definition, only isomeric transitions have been selected, so lifetimes cannot be considered typical. As seen, the electric dipole transitions are hindered by factors of 1×10^4 to 68×10^4. These factors are smaller than those observed for the $\frac{29}{2}^+$ (15^+) levels in the ^{203,205,207}Bi (^{206}Bi) isotopes, where the hindrance ranges from 3×10^6 to 11×10^6 (Refs. 30–33).

The observed hindrance factors for $E2$ transitions vary by almost three orders of magnitude (Table III), with the largest hindrances occurring in the $N=128$ isotones, ^{212}Rn, ^{213}Fr, and ^{214}Ra. These nuclei are in the middle of the $h_{9/2}$ shell and the Bogolubov-Valatin reduction factor reduces the $B(E2)$ values within the $h_{9/2}$ shell [Ref. 34, Eq. (59)]:

$$B(E2)\propto (U_{h_{9/2}}{}^2-V_{h_{9/2}}{}^2)\langle h_{9/2}||0(E2)||h_{9/2}\rangle \ .$$

The hindrance factors are, hence, a measure of the admixtures in the wave functions. When two valence neutrons are added, the hindrance of the $N=128$ isotones decreases relative to the $N=126$ isotones by roughly a factor of 10, as reflected in the small hindrances for ^{214}Rn and ^{216}Ra (Table III). This is because the neutron part of the transition is not appreciably affected by the blocking.

For $E3$ transitions, there are allowed single particle transitions for both protons and neutrons, viz.,

$$\pi i_{13/2}\rightarrow \pi f_{7/2}$$

and

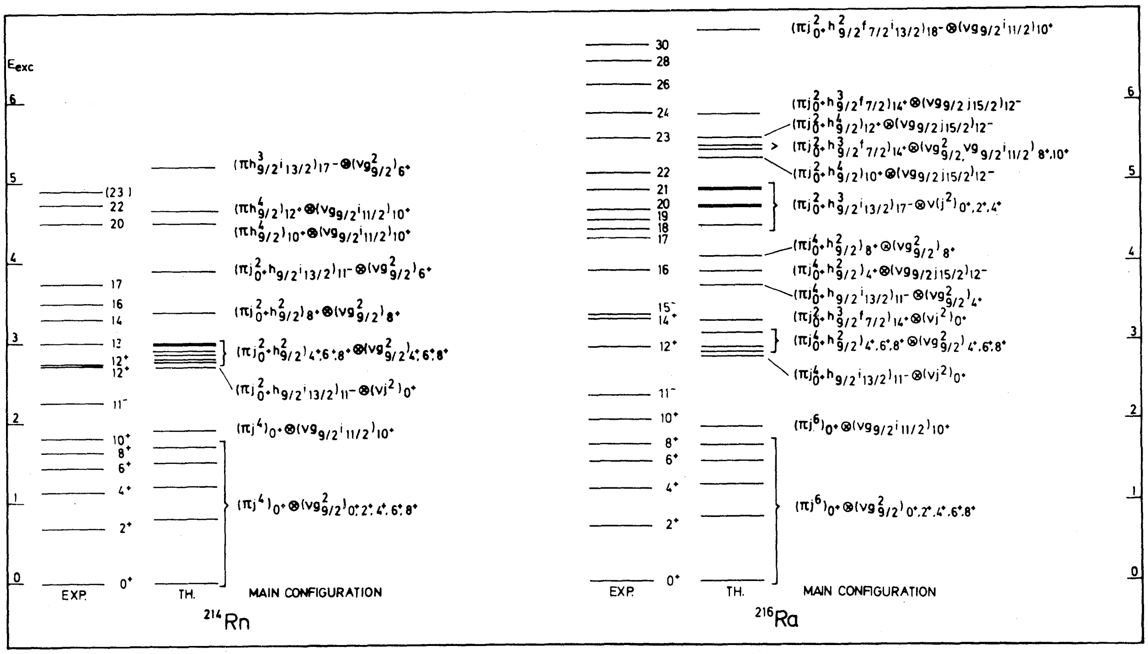

FIG. 9. The theoretical and experimental yrast levels of ^{214}Rn and ^{216}Ra. The zeroth-order energies are included for comparison.

$$\nu j_{15/2} \rightarrow \nu g_{9/2} \; .$$

As is known, however, the first excited state in the ^{208}Pb core is a collective octupole, with a $B(E3)$

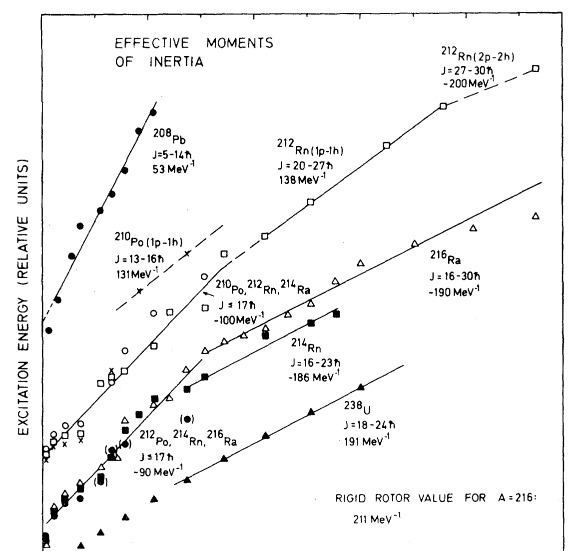

FIG. 10. Excitation energy as a function of $J(J+1)$. The slopes determine the effective moments of inertia. States in ^{208}Pb, $N=126$ isotones, $N=128$ isotones, and ^{238}U are displayed. The excitation energies are offset by 1 MeV for each group in order to make the picture clear.

value of 32 W.u. This state is known to couple strongly to allowed single-particle orbitals. The main components of the collective 3^- state at 2.61 MeV are[35,36]

$$0.42h_{9/2}d_{3/2}{}^{-1} - 0.30f_{7/2}s_{3/2}{}^{-1} + 0.25i_{13/2}h_{11/12}{}^{-1}$$

for protons, and

$$0.43g_{9/2}p_{3/2}{}^{-1} - 0.38i_{11/2}f_{5/2}{}^{-1} - 0.26j_{15/2}i_{13/2}{}^{-1}$$

for neutrons. The coupling of an odd nucleon to the 3^- vibration results in configuration mixing for some states. The coupling strengths are as follows[36]:

$$\pi: \; f_{7/2} \rightarrow 0.90f_{7/2} + 0.10(i_{13/2} \otimes 3^-)_{7/2^-}$$

$$i_{13/2} \rightarrow 0.85i_{13/2} + 0.14(f_{7/2} \otimes 3^-)_{13/2^-} \, ,$$

$$\nu: \; g_{9/2} \rightarrow 0.95g_{9/2} + 0.05(j_{15/2} \otimes 3^-)_{9/2^+}$$

$$j_{15/2} \rightarrow 0.77j_{15/2} + 0.23(g_{9/2} \otimes 3^-)_{15/2^-} \, .$$

Comparing these admixtures with the collectivities given in Table III, and remembering that the collectivity of the 3^- state is 32 W.u., one can draw the following conclusions. The two known $E3$ transitions in ^{210}Po ($11^- \rightarrow 8^+$ and $16^+ \rightarrow 13^-$) are essentially $i_{13/2} \rightarrow h_{9/2}$ single particle transitions, the excess transition probability being attributed to the admixed amplitude of $0.14(f_{7/2} \otimes 3^-)_{13/2^+}$. This is also reflected in their $B(E3)$ values. The $11^- \rightarrow 8^+$

TABLE III. Electromagnetic hindrance factors for $E1$, $E2$, and $E3$ transitions in proton- and/or neutron-particle nuclei of ^{208}Pb region.

Multipole	Nucleus[a]	E_γ (keV)	$J_i \rightarrow J_f$	$t_{1/2}$ (exp)	Hindrance[b]	Comment
$E1$	^{211}Po	193	$\frac{1}{2}^+ \rightarrow \frac{1}{2}^-$	3.5 ns	1.3×10^5	
	^{212}At	184	$11^+ \rightarrow 10^-$	21 ns[c]	6.8×10^5	
	^{212}At	278	$13^- \rightarrow 12^+$	<1 ns	$<1.1\times10^5$	
	^{213}Fr	787	$\frac{49}{2}^{(+)} \rightarrow \frac{47}{2}^-$	7 ns	1.8×10^7	Core excitation
	^{214}Rn	300	$14 \rightarrow 13$	<4 ns	$<5.6\times10^5$	
	^{216}Ra	52	$15^- \rightarrow 14^+$	<7 ns	$<1\times10^4$	
$E2$	^{210}Po	84	$8^+ \rightarrow 6^+$	115 ns	1.02	
	^{212}Rn	138	$6^+ \rightarrow 4^+$	165 ns	3.15	
	^{212}Rn	476	$14^+ \rightarrow 12^+$	8 ns	27	
	^{212}Rn	736	$27^- \rightarrow 25^-$	14 ns	412	Core excitation
	^{212}At	70	$5^- \rightarrow 3^-$	33 ns	0.4	Also neutron transition
	^{212}At	75	$15^- - 13^-$	37 ns	0.4	Also neutron transition
	^{213}Fr	179	$\frac{21}{2}^- \rightarrow \frac{17}{2}^-$	510 ns	22	
	^{213}Fr	94	$\frac{45}{2}^- \rightarrow \frac{41}{2}^-$	14 ns	0.14	
	^{214}Ra	179	$6^+ \rightarrow 4^+$	32 ns	2.2	
	^{214}Ra	221	$14^+ \rightarrow 12^+$	285 ns	29	
$E2$	^{214}Rn	183	$8^+ \rightarrow 6^+$	9 ns	0.45	Also neutron transition
	^{214}Rn	180	$16 \rightarrow 14$	95 ns	4.5	
	^{216}Ra	203	$8^+ \rightarrow 6^+$	8 ns	0.56	Also neutron transition
					Enhancement[d]	
$E3$	^{210}Po	1292	$11^- \rightarrow 8^+$	24 ns	3.1	
	^{210}Po	686	$16^+ \rightarrow 13^-$	~3 μs	2.1	Core excitation
	^{211}Po	1065	$\frac{15}{2}^- \rightarrow \frac{9}{2}^+$	14 ns	21	"Neutron transition"
	^{212}Rn	968	$25^- \rightarrow 22^+$	18 ns	31	Core excitation
	^{212}Rn	701	$30^+ \rightarrow 27^-$	154 ns	35	Core excitation
	^{213}Fr	681	$\frac{29}{2}^+ \rightarrow \frac{23}{2}^-$	238 ns	28	
	^{214}Rn	769	$20 \rightarrow 17$	230 ns	12	"Neutron transition?"
	^{214}Ra	817	$11^- \rightarrow 8^+$	333 ns	5.5	
	^{214}Ra	668	$17^- \rightarrow 14^+$	230 ns	33	

[a]Levels of ^{210}Po from Ref. 28, ^{211}Po from Ref. 29, ^{212}Rn, ^{213}Fr, and ^{214}Ra from Ref. 5, and ^{214}Rn and ^{216}Ra from the present work.
[b]$t_{1.2}$ (W.u.)/$t_{1/2}$ (Exp).
[c]Partial half-life of level.
[d]$t_{1/2}$ (Exp)/$t_{1/2}$ (W.u.).

transition in ^{214}Ra is of the same type, the difference being four additional protons coupled to $J^\pi=0^+$. As expected, the $B(E3)$ values are almost the same. All the other $B(E3)$ values in Table III are large (on the average 27 W.u.), and nearly equal to that of the collective octupole. As seen in the wave functions of Ref. 7, the $25^- \rightarrow 22^+$ and $30^+ \rightarrow 27^-$ transitions in ^{212}Rn may be understood as $\pi i_{13/2} \rightarrow \pi f_{7/2}$ and $\nu j_{15/2} \rightarrow \nu g_{9/2}$ effective "single particle" or 3^- transitions and thus the very large collectivities would be well explained. It should be noted that arguments for[37] and against[38] alternative 2-particle—2-hole configurations have been advanced for the $J^\pi=27^-$ and 30^+ states. Recent work by Dracoulis *et al.*, gives 24 single-particle units for a corresponding transition in ^{211}Rn.[38] Both the transitions $\frac{29}{2}^+ \rightarrow \frac{23}{2}^-$ in ^{213}Fr and $17^- \rightarrow 14^+$ in ^{214}Ra are of the type $\pi i_{13/2} \rightarrow \pi f_{7/2}$ and thus can attain large collectivities from the 3^- admixture in the wave function. In comparison with the above $B(E3)$ values, the $20^+ \rightarrow 17^-$ transition in the $N=128$ nucleus ^{214}Rn

TABLE IV. Theoretical alpha-decay half-lives[a] in ^{214}Rn and ^{216}Ra compared to experimental partial half-lives (lower limits).

I_i	I_f	E_α (MeV)	$t_{1/2}^{\alpha}$ (ns) Theor.	Exp.	L
^{214}Rn→^{210}Po					
8^+	0^+	10.7	140	~100	8
8^+	8^+	9.2	260	≥180	0
16	8^+	11.0	125	>500	8
16	11^-	9.7	210	>500	5
^{216}Ra→^{212}Rn					
8^+	0^+	11.1	90	920	8
8^+	8^+	9.4	180		0
24	11^-	12.5	60	>800	13[b]
24	17^-	11.2	90	>800	7[b]
24	20^+	9.8	150	>800	4[b]

[a]An explicit L dependence is suppressed. Since the angular momentum barrier tends to strongly retard large L values, theoretical values represent a lower limit.

[b]These values are constrained by the requirement that $(-1)^L$ give the proper change in parity. For a negative-parity spin 24 state, they should be one unit larger.

is somewhat slower, though it does agree with the prediction of the particle-core vibration model,[36] which gives a collectivity of about 10 W.u. Thus, considering all multipolarities, we find that to a large extent the experimental $B(EL)$ values in the $Z>82$ and/or $N>126$ region may be understood from a microscopic shell-model approach.

As was mentioned in Sec. IV, the α-decay rates cannot be calculated exactly because of the lack of a reliable theory. The absence of α branching can, however, be explained qualitatively. From the expression for Γ_α (Ref. 22) it is seen that, as a first approximation, the alpha width varies as the square of the alpha-particle energy. It can thus be expressed as

$$\Gamma_\alpha = K_\alpha (E_0 + E_i^* - E_f^*)^2 ,$$

where E_i^* (E_f^*) is the excitation energy of the initial (final) level (=0 for either ground state), and E_0 is the energy of the ground state of the mother nucleus relative to the daughter ($E_0=9.35$ MeV for ^{216}Ra→^{212}Rn and 9.08 MeV for ^{214}Rn→^{210}Po). Differences in recoil energies are omitted. The partial (alpha) half-life of an excited level, $t_{1/2}^{\alpha}$, is thus given by the expression

$$t_{1/2}^{\alpha} = [1+(E_i^* - E_f^*)/E_0]^{-4} t_{1/2}^{\alpha}(\text{g.s.}) ,$$

where $t_{1/2}$ (g.s.) is the ground state half-life (180 ns for ^{216}Ra and 270 ns for ^{214}Rn). Some examples of alpha-decay half-lives calculated with this expression are given in Table IV. They are compared to experimental partial half-lives and to lower limits deduced from nonobservation of certain α-decay channels. As seen, they generally agree to within an order of magnitude. It must be emphasized that the calculated results were derived under the simplifying assumption that the decay is configuration-independent (radial overlaps $=1$) and that all weight factors are unity. Since all these numbers should actually be less than unity and they enter squared in the denominator of $t_{1/2}$, the calculated values represent the lower limits. As seen in Table IV, some decays would involve large L values and would therefore be retarded by the angular momentum barrier.

ACKNOWLEDGMENTS

One of us (T.K.L.) is much indebted to E. Warburton and P. Thieberger at the BNL Van de Graaff facility for warm hospitality and excellent working conditions provided. He also gratefully acknowledges the financial support from Ellen ja Artturi Nyyssösen Säätiö in Jyväskylä and Ella och George Ehrnroots Fond in Helsinki. This work was supported by the Division of Basic Energy Sciences, DOE, under Contract Nos. DE-AC02-76CH00016 (BNL) and W-7405-eng-26 with the Union Carbide Corporation (Oak Ridge National Laboratory).

*Permanent address: Department of Physics, University of Jyväskylä, Nisulankatu 78, SF-40720 Jyväskylä 72, Finland.

†Present address: Schuster Laboratory, Dept. of Physics, University of Manchester, Manchester M13-9PL United Kingdom.

‡Permanent address: Oak Ridge National Laboratory, Oak Ridge, TN 37830.

[1]J. P. Schiffer and W. W. True, Rev. Mod. Phys. 48, 19 (1976).

[2]T. Lönnroth, thesis, University of Jyväskylä, Department of Physics, JYFL Research Report No. 3/1980 (unpublished).

[3]I. Bergström, J. Blomqvist, B. Fant, C. J. Herrlander, C.

G. Lindén, and K. Wikström, Proceedings of the Twelfth International Winter Meeting on Nuclear Physics, Villars, Switzerland, 1974.
[4]I. Bergström, Proceedings of the Sixteenth International Winter Meeting on Nuclear Physics, Bormio, Italy, 1978.
[5]D. Horn, O. Häusser, B. Haas, T. K. Alexander, T. Faestermann, H. R. Andrews, and D. Ward, Nucl. Phys. A317, 520 (1979).
[6]T. P. Sjoreen, U. Garg, and D. B. Fossan, Phys. Rev. C 21, 138 (1980).
[7]D. Horn, O. Häusser, T. Faestermann, A. B. McDonald, T. K. Alexander, J. R. Beene, and C. J. Heerlander, Phys. Rev. Lett. 39, 398 (1977); Proceedings of the International Conference on Nuclear Structure, Tokyo, 1977; J. Phys. Soc. Japan, Suppl. 44, 605 (1978).
[8]T. Lönnroth, University of Jyväskylä, Department of Physics, JYFL Research Report No. 4/1981 (unpublished).
[9]M. J. Martin, Nucl. Data Sheets 22, 545 (1977).
[10]T. P. Sjoreen, U. Garg, D. B. Fossan, J. R. Beene, T. K. Alexander, E. D. Earle, O. Häusser, and A. B. McDonald, Phys. Rev. C 20, 960 (1979).
[11]R. M. Lieder, J. P. Didelez, M. Beuscher, D. R. Haenni, M. Muller-Veggion, A. Neskakis, and C. Mayer-Böricke, Phys. Rev. Lett. 41, 742 (1978).
[12]K. Valli, E. K. Hyde, and J. Borggreen, Phys. Rev. C 1, 2115 (1970).
[13]K. Gono, K. Hiruta, T. Nomura, M. Ishihara, H. Utsunomiya, T. Sugitate, and K. Ieki, J. Phys. Soc. Jpn. 50, 377 (1981).
[14]T. Nomura, K. Hiruta, T. Inamura, and M. Odera, Nucl. Phys. A217, 253 (1973).
[15]T. Nomura, K. Hiruta, M. Yoshie, H. Ikezoe, T. Fukuda, and O. Hashimoto, Phys. Lett. 58B, 273 (1975).
[16]D. Horn, O. Häusser, and M. A. Lone (unpublished).
[17]A. deShalit and I. Talmi, *Nuclear Shell Theory* (Academic, New York, 1963).
[18]A. N. Wapstra and K. Bos, At. Data Nucl. Data Tables 19, 215 (1977).
[19]T. T. S. Kuo and G. H. Herling, Naval Research Laboratory Memorandum Report 2258, 1971.
[20]S. A. Moszkowski, in *Alpha-, Beta- and Gamma-Ray Spectroscopy*, edited by K. Siegbahn (North-Holland, Amsterdam, 1966), Vol. 2.
[21]J. Blomqvist and S. Wahlborn. Ark. Fys. 16, 545 (1960).
[22]S. G. Kadmenskij, V. E. Kalechits, and A. A. Martyrov, Yad. Fiz. 13, 300 (1971) [Sov. J. Nucl. Phys. 13, 166 (1971)]; Yad. Fiz. 16, 717 (1972) [Sov. J. Nucl. Phys. 16, 400 (1973)].
[23]J. O. Rasmussen, Nucl. Phys. 44, 93 (1973).
[24]R. M. Lieder, J. P. Didelez, H. Beuscher, D. R. Haenni, M. Müller-Veggian, A. Neskakis, and C. Mayer-Böricke, Phys. Rev. Lett. 41, 742 (1978).
[25]N. Auerbach and I. Talmi, Phys. Lett. 10, 297 (1964).
[26]N. K. Glendenning and K. Harada, Nucl. Phys. 72, 281 (1965).
[27]A. R. Poletti, G. D. Dracoulis, C. Fahlander, and A. Morrison, Nucl. Phys. A359, 180 (1981).
[28]B. Fant, Phys. Scr. 4, 175 (1972).
[29]B. Fant, T. Lönnroth, and V. Rahkonen, Nucl. Phys. A355, 171 (1981).
[30]H. Hübel, A. Kleinrahm, C. Günther, D. Me-tin, and R. Tischler, Nucl. Phys. A294, 177 (1978).
[31]R. Brock, C. Gunther, H. Hübel, A. Kleinrahm, D. Mertin, P. Meyer, and R. Tischler, Nucl. Phys. A278, 45 (1977).
[32]T. Lönnroth, L. Vegh, K. Wikström, and B. Fant, Z. Phys. A 287, 307 (1978).
[33]T. Lönnroth, J. Blomqvist, I. Bergström, and B. Fant, Phys. Scr. 19, 233 (1979).
[34]D. R. Bès and R. A. Sorensen, in *Advances in Nuclear Physics*, edited by M. Baranger and E. Vogt (Plenum, New York, 1969), Vol 2.
[35]V. Gillet, A. M. Green, and E. A. Sanderson, Nucl. Phys. 88, 321 (1966).
[36]I. Hamamoto, Phys. Rep. 10C, 63 (1974).
[37]K. Matsuyanagi, T. Døssing, and K. Neergaard, Nucl. Phys. A307, 253 (1978).
[38]G. D. Dracoulis, C. Fahlander, and A. R. Poletti, Phys. Rev. C 24, 2386 (1981).
[39]J. Gilat, Brookhaven National Laboratory Report No. BNL 50247 T-580, 1970 (unpublished), and references therein.